Topology of the secondary structure elements of ribosomal protein L7/L12 from *E. coli* in solution

E.V. Bocharov[a], A.T. Gudkov[b], A.S. Arseniev[a,*]

[a]*Shemyakin–Ovchinnikov Institute of Bioorganic Chemistry, Russian Academy of Sciences, ul. Miklukho-Maklaya, 16/10, Moscow, 117871, Russian Federation*
[b]*Institute of Protein Research, Russian Academy of Sciences, Pushchino, Moscow Region, Russian Federation*

Received 24 November 1995; revised version received 15 December 1995

Abstract Topology of the secondary structure elements of ribosomal protein L7/L12 has been studied. The sequential assignment was obtained for main and side chain resonances. This allows the overall secondary structure to be described. The results of high resolution NMR studies show that dimer of the ribosomal protein L7/L12 from *Escherichia coli* has a parallel (head-to-head) orientation of subunits, and N-terminal domain (NTD, residues Ser1–Ser33) has no contacts with the C-terminal domain (CTD, residues Lys51–Lys120). The NMR data for CTD are in line with crystallographic structure. The flexible interdomain (hinge) region (residues Ala34–Glu50) has an unordered structure, the Pro44 forming both *cis* and *trans* peptide bonds. Due to the conformational exchange the intensities of the peaks from the NTD are low. The conformation of the NTD, which is responsible for the formation of the L7/L12 dimer, is α-helical hairpin. The NTD dimer forms an antiparallel four-α-helix bundle.

Key words: Ribosome; L7/L12 protein; Sequence-specific NMR assignment; Secondary structure

1. Introduction

The 50S ribosomal subparticle contains four copies of the acidic protein L7/L12 (L7/L12 consists of 120 amino acid residues and L7 is the N-terminal acetylated form of L12) [1,2]. The protein L7/L12 is essential for efficient polypeptide synthesis in bacteria. It plays an important role in all factor dependent reactions of ribosomes (for a review see [3]). The protein L7/L12 is bound to the large ribosomal subunit via protein L10. In solution the protein L7/L12 exists as a dimer [4], and two such dimers are capable of further association with protein L10, forming pentameric $(L7/L12)_4L10$ complex [5]. The $(L7/L12)_4L10$ complex is in the vicinity of the ribosomal subunit interface (cavity), where the sites for binding of two L-shaped tRNA molecules on the ribosome are situated. While the N-terminal part of L7/L12 is responsible for binding onto the ribosome, the C-domain, on the other hand, seems to be a functional region, since it is crucial for inducing GTPase activity in EF-Tu and EF-G elongation factors. The L7/L12 protein has a fair mobility in the ribosome and it does not take part in association of ribosomal subunits. Hence the structure and the mobility of L7/L12 are relevant for the functioning of this protein during the translation process [6].

Various arrangements of the polypeptide chains in the L7/L12 dimer have been proposed: with head-to-tail and head-to-head orientation of monomers (reviewed in [3]). Recently the head-to-head orientation of the subunits in the dimer has been suggested in studies of functional activity of the L7/L12–Cys38 mutant dimer [7]. Oxidation of all the three (14, 17 and 26) methionine residues of L7/L12 disrupts its dimer structure [8,9]. The oxidized protein does not bind to the ribosome, though its C-terminal globular structure is preserved [10]. Besides, the L7/L12 dimer is unstable due to spontaneous proteolysis of the protein that produces two fragments containing residues Ser1–Ala36 and Ala47–Lys120. Only the tertiary structure of the CTD (residues Glu53–Lys120) was previously determined at 1.7 Å resolution by X-ray crystallography [11]. CTD is two-layer α/β-protein. Applying ^{1}H NMR technique to a number of L7/L12 mutants, as well as to monomeric and dimeric forms of the protein and to the CTD, certain resonances were identified and an extent of the flexible regions was assessed [12,13].

In this paper we report the nearly complete assignment of the ^{1}H and ^{15}N resonances of wild-type L7/L12 dimer by homonuclear and heteronuclear NMR techniques. Using NOE's, $^3J_{HN\alpha}$'s and hydrogen-deuterium exchange rates of backbone amide groups, we also outline the secondary structure and global fold of the protein.

2. Materials and methods

The protein was uniformly labeled with ^{15}N to overcome spectral overlap of proton resonances. The plasmid containing L7/L12 gene was grown in *E. coli* strain XL1 on minimal milieu with $^{15}NH_4Cl$. The ribosomes from crude cell extract were precipitated and the supernatant fraction was used for L7/L12 purification. The protein was isolated by ion-exchange chromatography on DE-cellulose using buffers with 6 M urea by a published procedure [5]. The protein samples isolated in denaturing conditions do not differ according to NMR data from L7/L12 obtained under 'native' conditions.

For the reason of spontaneous proteolysis of L7/L12, which is almost completed in 2–3 weeks, we needed 3 NMR samples (~1 mM concentration each) to collect all necessary NMR data. All NMR spectra were acquired at 30°C on a UNITY-600 Varian spectrometer. The buffer solutions containing 0.05 M sodium phosphate, 0.1 M KCl and either 10% D_2O + 90% H_2O (H_2O sample) or 99.9% D_2O (D_2O sample) were adjusted to pH meter readings of 6.9.

All NMR spectra were processed by VNMR (Varian) software and analyzed in XEASY program [14]. For prevention of saturation transfer from H_2O solvent to protein NH's, the solvent signal was suppressed

*Corresponding author. Fax: (7) (095) 335 71 03.
E-mail: aars@siobc.ras.ru

Abbreviations: NMR, nuclear magnetic resonance; 2D, two-dimensional; 3D, three-dimensional; NOE, nuclear Overhauser enhancement; DQF-COSY, 2D double quantum filtered correlated spectroscopy; NOESY, 2D NOE-correlated spectroscopy; TOCSY, 2D total correlated spectroscopy; HMQC, 2D ^{1}H-detected heteronuclear multiple quantum correlation; $^3J_{HN\alpha}$, spin–spin coupling constant of $HNC^{\alpha}H$ protons; jr, the jump-and-return method of solvent signal suppression; CTD, C-terminal domain; NTD, N-terminal domain.

SSDI 0014-5793(95)01531-0

by application of jump-and-return (jr) technique with a weak presaturation pulse (field strength 25 Hz) during the relaxation delay of 1.4 s. Residual solvent signal was removed from the final spectrum by convolution of the time domain data during data processing.

The resonances of the L7/L12 dimer (M_r = 25 kDa) are too broad for application of the 2D ^{1}H NMR technique for the complete identification of spin systems of amino acid residues, therefore proton 2D spectra were used as an additional source to the sequence-specific resonance assignment and for more accurate definition of chemical shifts. TOCSY experiments were performed with mixing periods of 30 or 70 ms for H_2O sample and of 40 ms for D_2O sample. DQF-COSY and NOESY (mixing time of 70, 100, and 180 ms) spectra of L7/L12 were acquired for H_2O and D_2O samples. After applying Gaussian filter, zero filling, Fourier transformation and baseline correction the final data matrices were 2048(complex) × 4096(complex) points.

Heteronuclear, proton-detected experiments were carried out to make ^{15}N resonance assignments and to measure the $^3J_{HN\alpha}$'s. All 2D ^{1}H-^{15}N HMQC spectra were acquired using standard methods [15] with ^{15}N-dimension spectral width of 2000 Hz for the whole spectrum and 1400 Hz for wrapped up spectrum to increase spectral resolution. 5 HMQC spectra recorded in 0.8, 1.6, 2.4, 3.2, and 4 h (complete exchange) after solubilization of lyophilized sample in 99.9% D_2O at 30°C were used to qualitatively determine deuterium exchange rates of amide protons.

The heteronuclear 3D TOCSY-jr-HMQC (mixing period of 50 ms) and NOESY-jr-HMQC (mixing time of 100 ms) spectra [16,17] were run consecutively in order to minimize differences in sample conditions. Additional 3D NOESY-jr-HMQC and HMQC-NOESY-jr-HMQC spectra of the next sample of L7/L12 were obtained with mixing time of 180 and 100 ms, respectively. For spectra based on detection of amide protons, the aliphatic halves of the spectra were discarded. The spectra were derived from a 128(complex) × 32(complex) × 1024(complex) data matrix, and after processing the final matrices consisted of 256 × 64 × 512 real points.

^{1}H chemical shifts are given relatively to an internal standard sodium 2,2-dimethyl-2-silapentane-sulfonate. ^{15}N chemical shifts are measured with respect to an external standard containing 2.9 M $^{15}NH_4Cl$ in 1 M HCl (24.93 ppm).

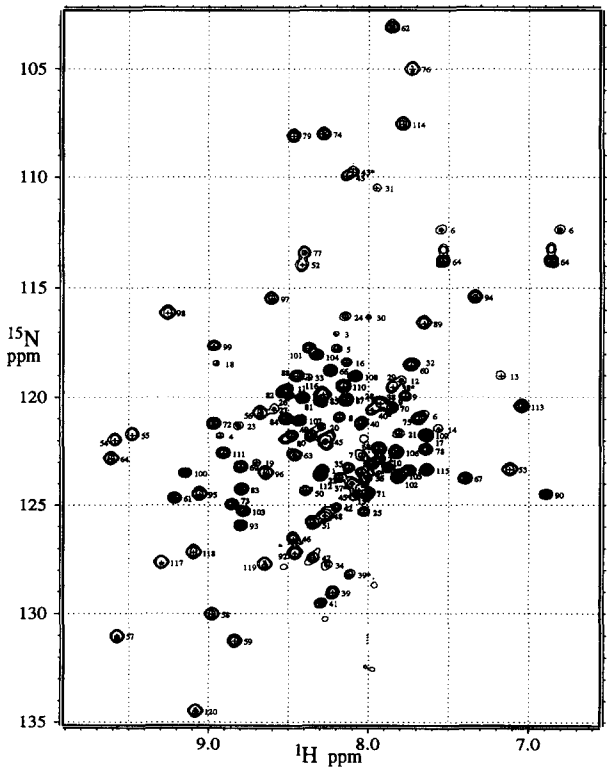

Fig. 1. ^{1}H-^{15}N HMQC spectrum of uniformly ^{15}N-labeled L7/L12 dimer recorded at pH 6.9 and 30°C. The ^{1}H-^{15}N backbone resonance assignments are indicated by numbers.

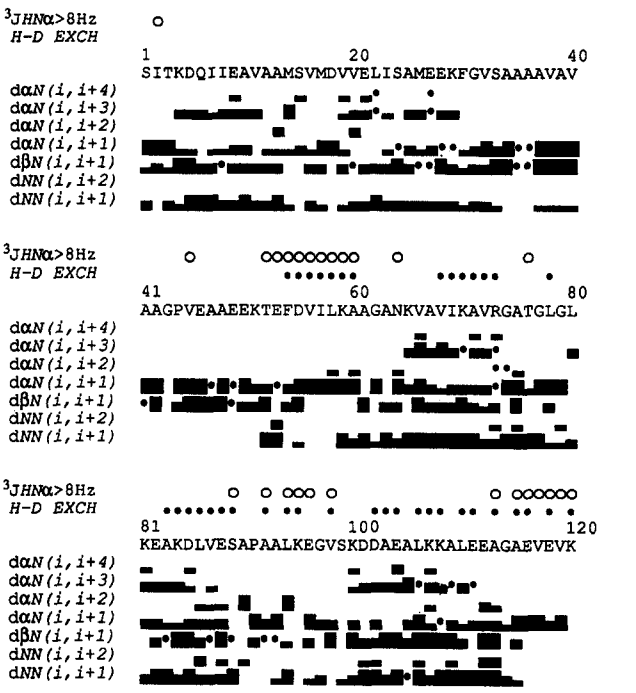

Fig. 2. Summary of the sequential and medium-range NOE's in the L7/L12 protein. The observed NOE's classified as strong, medium and weak are shown by thick, medium and thin lines, respectively. If the presence of cross-peak is somewhat doubtful, it is indicated by a black circle. The residues with the slowly exchanging NH protons are indicated by solid circles above the sequence. Open circles indicate residues with $^3J_{HN\alpha}$>8 Hz.

3. Results and discussion

3.1. Sequence-specific resonance assignment

Standard procedures were used for sequential resonance assignments [18]. A combination of 3D TOCSY-HMQC and 3D NOESY-HMQC jr experiments in H_2O allowed for the identification of spin systems with through-bond correlations and through-space connectivities. In places where the NH-NH sequential NOE was not observed due to the amide proton resonances of both NH's being similar, connectivities were made using the HMQC-NOESY-HMQC experiment. Once stretches of connectivities between amino acid spin-systems were found, the chains of spin-system identities were fitted into the sequence of L7/L12. Connectivity stretches in the NTD of L7/L12 were sometimes interrupted due to weak or ambiguous NOE's. At the end of the assignment, the remaining spin-systems were inserted into the sequence by a process of elimination. In this way, all cross-peaks in the HMQC spectra were fitted into the sequence of L7/L12 (Fig. 1).

The NH/C$^\alpha$H fingerprint region as well as aliphatic part of TOCSY spectrum of L7/L12 showed generally well dispersed cross peaks of CTD and very poor dispersion for the weak peaks of NTD. The HMQC spectrum of L7/L12 (Fig. 1) shows well resolved chemical shifts in the ^{15}N dimension. Most of the ^{15}NH backbone cross peaks and all cross-peaks of the $^{15}NH_2$ side chains (Gln6 and Asn64 residues) are present. (The peaks of $^{15}NH_2$ side chain groups are forking in the ^{15}N dimension due to isotope chemical shift resulting from presence of 10% D_2O). HMQC spectrum (Fig. 1) contains mixture of weak and strong

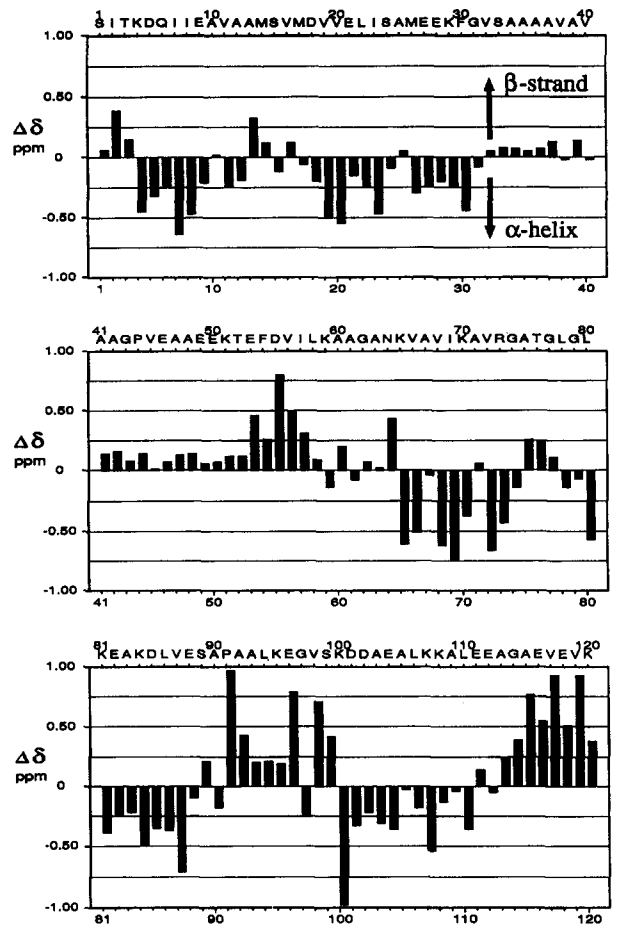

Fig. 3. Comparison of backbone $C^{\alpha}H$ chemical shifts of the L7/L12 residues (horizontal axis) at *trans* configuration of Gly43–Pro44 peptide bond with random coil values (vertical axis). The arrows display a tendency of α-proton chemical shift, $\Delta\delta = \delta_{L7/L12} - \delta_{random\ coil}$, for β-strand and α-helix backbone conformations of a protein.

peaks. It can be surmised from the assignment that the strong peaks correspond to CTD and hinge region residues while weak peaks – to NTD residues.

The configuration of X–Pro peptide bond of the two proline residues was determined by examining the 2D homonuclear spectra as in [19]. Strong $d_{\alpha\alpha}(i,i+1)$ NOE between Ala90 and Pro91 indicates *cis* configuration of Ala90–Pro91 peptide bond. In the case of Pro44 the situation is complex. The high mobility of the hinge region, combined with the small energy difference between *cis* and *trans* configurations of X–Pro peptide bond, gives rise to the slow interconversion of *cis* and *trans* alternative forms of Gly43–Pro44 peptide bond. Strong $d_{\alpha\delta}(i,i+1)$ NOE between major Gly43 and Pro44, as well as $d_{\alpha\alpha}(i,i+1)$ NOE between minor Gly43 and Pro44 evidence that both *trans* and *cis* configurations of Gly43–Pro44 peptide bond are present. Basing on the relative volumes of the major and minor Gly43 peaks in the HMQC spectrum the *trans*/*cis* ratio is about 2/1. In the HMQC spectrum the many cross-peaks from hinge region are doublet, some of them fail to be assigned uniquely.

Analysis of the 2D and 3D NOESY experiments gave rise to the specific pattern of the NOE connectivities (Fig. 2) indicating the secondary structure of L7/L12. Stretches of $d_{NN}(i,i+1)$, $d_{\alpha N}(i,i+3)$ and $d_{\alpha N}(i,i+4)$ connectivities are characteristic of α-helical regions. Stretches of strong $d_{\alpha N}(i,i+1)$ connectivities are characteristic of extended strands. The β-structure was further evaluated *via* the long-range $d_{\alpha N}(i,j)$ and $d_{NN}(i,j)$ connectivities between the β-strands [18]. Additional qualitative information on secondary structure was obtained from $^3J_{HN\alpha}$'s and hydrogen-deuterium exchange rates of amide groups. $^3J_{HN\alpha}$'s under 6 Hz are characteristic of helical configuration, while those over 8 Hz are indicative of an extended backbone configuration. Amide protons, that exchange relatively slower when the protein was placed in a D_2O buffer, are thought to be either involved in stable hydrogen bonds or significantly shielded

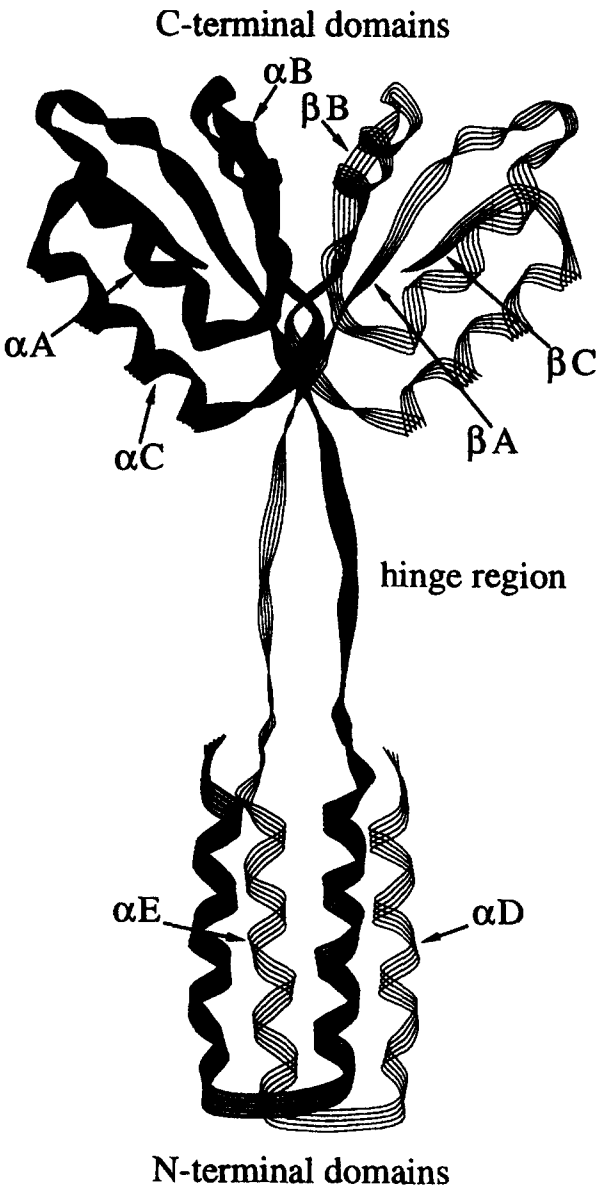

Fig. 4. Ribbon diagram of the L7/L12 dimer structure drawn based on secondary structure analysis and long range NOE's. In this diagram N-terminal four-α-helix antiparallel bundle (residues from Ser1 to Ser33) situated at the bottom of the figure. The hinge region includes the highly mobile Ala34–Glu50 residues. The NMR data for the CTD's (residues from Lys51–Lys120) are in line with X-ray data [11]. CTD consists of three antiparallel β-strands (βB-βA-βC) in one layer and three α-helices (αB-αA-αC) in another one. The figure was generated with the program SYBYL (TRIPOS Associates Inc.).

from solvent. Fig. 2 shows a summary of all this information. As it is readily observed, all residues with the slowly exchanging NH protons are from CTD.

It has been shown that the difference between $C^{\alpha}H$ proton chemical shift of a given residue and its random coil value can indicate the type of secondary structure in the place of given residue in the folded protein [20]. The difference tends to be positive (ranging from 0.34 to 0.66 ppm) for residues in an extended strand conformation and negative (ranging from 0.15 to 0.60 ppm) for those in helical conformation. Comparison of the $C^{\alpha}H$ chemical shifts for L7/L12 with typical random coil values [20] is shown in Fig. 3. The data agree closely with the secondary structure defined by sequential and medium-range NOE's, hydrogen–deuterium exchange data and analysis of $^{3}J_{HN\alpha}$'s (Fig. 2).

Although accurate definition of the start and the end of secondary structure elements requires further analysis, the data suggest the following features. The stable CTD, comprising residues Glu51–Lys120, consists of three β-strands (βA, residues Phe54–Ala60; βB, residues Ala92–Val98; βC, residues Ala115–Lys120) and three α-helices (αA, residues Lys65–Gly74; αB, residues Leu80–Val87; αC, residues Lys100–Glu112). The long range $d_{\alpha N}(i,j)$ and $d_{NN}(i,j)$ connectivities between βA and βB strands and between βA and βC revealed antiparallel β-layer (βB-βA-βC) in agreement with the X-ray data [11]. The flexible hinge region includes residues from Ala34 to Glu50. The NTD, formed by residues from Ser1 to Ser33, incorporates two well-defined α-helices (αD, residues Lys4–Ala12, and αE, residues Val19–Gly31).

When secondary structure was defined, it is possible to determine the global fold, basing on the long range NOE's. Between CTD and NTD the NOE's were not observed. In the CTD a number of long range NOE's between the secondary structure elements were observed: between αA and αC, αA and αB, αC and βC. The NOESY and NOESY-jr-HMQC spectra with a mixing time of 100 and 180 ms having been examined, a number of intermolecular contacts was detected between regions of residues 77–79 and 93–96. All the data are in line with the X-ray structure of the CTD dimer [11], which indicates that the residues 77–79 may form a small β-strand neighboring and antiparallel to βB. A few long range NOE's were found between αD and αE helices in NTD's. Being regarded as merely intramolecular, the observed NOE's are contrary to the obtained secondary structure. Consequently, these long range NOE's of the NTD dimer are sums of inter- and intramolecular contacts. At the same time the contacts (such as Phe30 with Gln6, Ile7, Ile8) fit to the antiparallel alignment of four α-helices but exclude the parallel alignment.

The data obtained show, that except the hinge region near Pro44 having two configurations, all identical amino acid residues from two polypeptide chains in the L7/L12 dimer have equivalent environments, since no bifurcations of NTD and CTD cross-peaks were detected. Consequently, the structure of the L7/L12 dimer is a symmetrical one.

The NMR and X-ray data, the symmetrical structure of the dimer and the dimerisation via NTD's allow to define a tentative topology for the secondary structure elements of the L7/L12 dimer (Fig. 4). The CTD's do not interact with the NTD's, but are connected to them by the flexible hinge. The NTD is an α-helical hairpin, and two of them form an antiparallel four-α-helix bundle. Resulting from long range NOE contacts the Phe30 ring should be directed inward the bundle. Besides, two rings of Phe30 having upfield shifted resonances of C-2,6 protons and downfield shifted resonances of C-3,5 protons (what is not common) possibly interact with each other. These confirm the data in [10], that the Phe30 participates in intermolecular interaction and might stabilize the L7/L12 dimer structure.

As noted above, the NTD residues have weak cross peak intensities in NMR spectra. It is an indicator of an internal conformational exchange process in millisecond time scale in the four α-helices bundle motif of the dimer. The exchange process may have a functional/structural significance for binding to protein L10.

In the subsequent NMR study we shall resolve the structure of the L7/L12 dimer in solution using the obtained resonance assignments. As two of the L7/L12 dimers are bounding to the ribosome *via* protein L10, it would be also worthwhile studying the extremely tight interaction of L7/L12 with the protein L10 in solution.

The ^{1}H and ^{15}N chemical shifts from ribosomal protein L7 *E.coli* are available on ftp site: *ftp.siobc.ras.ru*.

Acknowledgements: The authors express their sincere thanks to Dr. V.N. Bushuev and Dr. A.Liljas for helpful discussions. We thank O.I. Gryaznova and L.I. Vasilieva for preparing of the protein samples used. This work was supported by Grant94-04-12051a from Russian Foundation for Fundamental Research and by Grant J6D100 from ISF and Government of Russian Federation.

References

[1] Subramanian, A.R. (1975) J. Mol. Biol. 95, 1–8.
[2] Hardy, S.J.S. (1975) Mol. Gen. Genet. 140, 253–279.
[3] Liljas, A. (1982) Progr. Biophys. Mol. Biol. 40, 253–279.
[4] Möller, W., Schrier, P.I., Maassen, J.A., Zantema, A., Schop, E., Reinalda, H., Cremers, A.M.F. and Mellema, J.E. (1983) J. Mol. Biol. 163, 533–549.
[5] Möller, W., Groene, A., Terhost, C. and Amons, R. (1972) Eur. J. Biochem. 25, 5–12.
[6] Pettersson, I., Hardy, S.J.S. and Liljas, A. (1976) FEBS Lett. 64, 135–138
[7] Gudkov, A.T., Budovskaya, E.V. and Sherstobaeva, N.M. (1995) FEBS Lett. 367, 280–282.
[8] Gudkov, A.T., Behlke, J., Vtiurin, N.N. and Lim, V.I. (1977) FEBS Lett. 82, 125–129.
[9] Caldwell P., Luk D.c., Weissbach H. and Brot, N. (1978) Proc. Natl. Acad. Sci. USA 75, 5349–5352.
[10] Gudkov, A.T., Khechinashvili, N.N. and Bushuev, V.N. (1978) Eur. J. Biochem. 90, 313–318.
[11] Leijonmarck, M. and Liljas, A. (1987) J. Mol. Biol. 195, 555–580.
[12] Bushuev, V.N., Gudkov, A.T., Liljas, A. and Sepetov, N.F. (1989) J. Biol. Chem. 264, 4498–4515.
[13] Bushuev, V.N., Sepetov, N.F. and Gudkov, A.T. (1984) FEBS Lett. 178, 101–104.
[14] Bartels, C., Xia T.H., Billeter, M., Güntert, P. and Wüthrich, K. (1995) J. Biomol. NMR 5, 1–10.
[15] Bax, A., Mitsuhiko, I., Kay, L.E., Torchia, D.A. and Tschudin, R. (1990) J. Magn. Reson. 86, 304–318.
[16] Summers, M. F., Marzilli, L. G. and Bax, A. (1986) J. Am. Chem. Soc. 108, 4285–4294.
[17] Ikura, M., Bax, A., Clore, G.M. and Gronenborn, A.M. (1990) J. Am. Chem. Soc. 112, 9020–9022
[18] Wüthrich, K. (1986) NMR of Proteins and Nucleic Acids, Wiley, New York.
[19] Hinck, A.P., Eberhardt, E.S. and Markley, J.L. (1993) Biochemistry 32, 11810–11818.
[20] Wishart, D.S., Sykes, B.D. and Richards, F.M. (1991) J. Mol. Biol. 222, 311–333.